Journal of Cell and Animal Biology Vol. 5(2), pp. 33-40, February 2011
Available online at http://www.academicjournals.org/JCAB
ISSN 1996-0867 ©2011 Academic Journals

Full Length Research Paper

Purification and characterizations of NAD dependent isocritrate dehydrogenase from human kidney mitochondria

Mukaram Shikara

Biotechnology Division, Department of Applied Sciences, University of Technology, Baghdad, Iraq.
E-mail: mukaramshikara2010@yahoo.com.

Accepted 2 February, 2011

NAD-IDH (Nicotinamide adenine dinucleotide socitric dehydrogenase) has been purified in 1216-fold with a total recovery of 7.5% from the mitochondria of human kidney by using a combination of affinity chromatography with the anion-exchange matrix that allowed obtaining a preparation of high purity. The shape of the peak from Sephacryl S-100 and the results from SDS-PAGE confirm that the enzyme is a tetramer with subunits of 80,000 each, and a native molecular mass of about 320,000. The enzyme shows activity in the absence of any divalent metal ions, but Mn^{+2} is a better activator than Mg^{+2} at lower concentrations (0.5 mM), but it will inhibit the enzyme at higher concentrations (2 mM). ATP (Adenosine triphosphate) and NADH inhibit the enzyme competitively according to Lineweaver-Burk plot. The NAD-IDH does not indicate a homotropic cooperative effect of isocitrate in either the absence or presence of ADP. Increasing concentrations of NAD decrease the Km of isocitrate while increasing levels of isocitrate lower the Km of NAD. Km of either isocitrate or NAD is lowered further in the presence of ADP. The inhibition by ATP (or NADH) cannot be counteracted by ADP in the presence of isocitrate, so ADP cannot enhance NAD-IDH activity nor reverse inhibition by ATP (or NADH), while isocitrate will bind to the enzyme and prevent it from interacting with ADP. The activity of NAD-IDH in mitochondria is probably controlled in a complex way by NADH, ATP and divalent ions.

Key words: Nicotinamide adenine dinucleotide socitric dehydrogenase, isocitrate, Adenosine triphosphate, Nicotinamide adenine dinucleotide hydrogenase, human kidney, purification.

INTRODUCTION

Isocitrate dehydrogenases (IDH) are enzymes in tricarboxylic acid cycle (TCA) that catalyze oxidative decarboxylation of isocitrate to a-ketoglutarate using NAD or NADP as cofactor and widely distributed in the three domains of life: archaea, bacteria and eukaryotes (Karlstrom et al., 2005). NAD-dependent IDH is localized in mitochondria matrix, while NADP–IDH is localized in both mitochondria and cytoplasm. The biochemical knowledge of NAD-IDH is much less advanced comparing with NADP-IDH since it has been difficult to work with NAD-IDH than NADP-IDH enzyme. The distinct function of NAD-IDH is its ability to recognize its respective substrates and coenzyme (Chen and Jeong, 2000). To our knowledge, no NAD-IDH from eukaryotic organisms has yet been purified to homogeneity but several researchers purified partially NAD-IDH from the mitochondria of several eukaryotes such as potato mitochondria (Tezuka and Laties, 1983), mitochondria from blowfly muscles (Wadano et al., 1989), mitochondria of higher plants (Chen and Gadal, 1990), and pea mitochondria (Oliver and McIntosh, 1995).

The regulatory importance of NAD-IDH is still under debate. The present paper is dealing with the properties of NAD-IDH enzyme purified from the mitochondria that was isolated from human's kidney.

MATERIALS AND METHODS

50 g of human kidney from 20 years old assassinated female had been obtained from Department of Forensic Medicine and Pathology, Faculty of Medicine, University of Jordan, Amman, Jordan. Standard proteins, DEAE-Sepharose, DEAE-Sephacel,

Sephacryl S-100 were purchased from Sigma. Molecular weight markers were obtained from Boehringer, Mannheim, Germany. Motor driven tightly fitting glass/Teflon Potter Elvehjem homogenizer (30 mL). Buffer A consisted of 0.05 M Tris/MOPS and 12.1 g of 1 M sucrose. The mixture was brought to 1 L of distilled water and adjusted to pH 7.5. It was stored at 4°C, while buffer B consisted of 0.05 M Tris/MOPS and brought to 1 L of distilled water and adjusted to pH 7.5 and stored at 4°C (if ADP is used, the pH will be adjusted to 8.2). All glassware were washed three times with distilled water to avoid Ca^{2+} contamination. Ca^{2+} overloaded was the most common cause for the dysfunction of isolated mitochondria.

All buffers were prepared in the same day of the experiment to avoid bacterial/yeast growth in stored buffers, and since pH depended on temperature, the pH must be measured in all solutions at 25°C.

Purification of mitochondria

Mitochondria were purified according to the method of Frezza et al. (2007) as modified by Gregg et al. (2009) from human kidney. The kidney was rinsed free of blood by using ice-cold buffer A and minced into small pieces using scissors. The buffer used during the mincing was discarded and replaced with 5 mL of ice-cold fresh buffer A. The suspension was transferred into a Teflon pestle and homogenized at 1,600 g at 4°C to minimize activation of damaging phospholipases and proteases for few minutes. All other harsher techniques, including glass pestle in a glass potter, could easily damag the mitochondria. The optimal ratio between tissue and isolation buffer ranges from 1:5 to 1:10 (w: v). The homogenate was transferred into a 50 mL polypropylene Falcon tube and centrifuged at 600 g for 10 min at 4°C. The pellet (contained the cell debris and nuclei) was discarded. The supernatant (contained all the lighter cellular fractions) was centrifuged at 5,000 g for 20 min at 4°C in chilled centrifuge tubes. The supernatant (contained microsomes, membrane fragments, ribosomes and cytoplasmic enzymes) was decanted and the pellet (contained crude mitochondria) was resuspended in 12 mL of ice-cold buffer A.

The re-suspension was enriched in mitochondria which mixed with other organelles such as “golgi” apparatus, endoplasmic reticulum and vacuoles. In order to obtained pure mitochondria, this re-suspension was loaded onto a 4 mL each of 15, 23, 32 and 60 wt: v step sucrose density gradient prepared in the aforementioned buffer and centrifuged at 100,000 g in a SW60Ti rotor (Beckman Ultra centrifuge tube) for 5 h at 4°C. Fractions were then collected from the bottom of the gradient. The intact mitochondria form a brown band at the 60 to 32% sucrose interface and removed gently by using a pipette with a cut tip and placed into a separate Beckman centrifuge tube which was filled with buffer A. The semi-pure mitochondria were centrifuged for 30 min at 10,000 g at 4°C, and the supernatant was decanted, while the precipitate consisted of pure mitochondria was used for the next step. The mitochondria should not be diluted with buffer in order to retain their functionality for a longer time.

The concentration of mitochondria in this preparation is about 80 $mg.mL^{-1}$ with the total volume is about 1 mL.

Assays for mitochondria

To identify the mitochondria, slides were prepared from all samples and a drop of methyl green pyronin was added and all slides observed at 400X with bright field: nuclei should stain green, cytoplasm red or pink, and mitochondria can be seen as small dots and protein concentration of each fraction was measured (Kurnick and Mirsky, 1950). Another method for identification of mitochondria is to use the blue dye 2,6 dichlorophenol indolphenol (DCPIP). A mixture of 1 mL of 0.1 M succinate, 1 mL of 5 mM KCN, 1 mL of mitochondrial preparation and 4 mL 0.05 M phosphate buffer (pH 7.5) were mixed and left for 5 min at 25°C. 1 mL of 70 uM DCPIP, 0.3% (w: v) was added to the mixture and read after 5 min at 600 nm. DCPIP will accept an electron from NADH (inside mitochondria) and becomes a reduced colourless form.

Isolation and purification of NAD-IDH

Mitochondrial preparation was thawed at room temperature and was layered onto a 1.5 x 40 cm DEAE-Sepharose column that was previously equilibrated with 4 L of buffer A. About 70% of the enzyme activity was eluted in the second peak at 0.55 M NaCl. The active fractions from the second peak were pooled and dialyzed for 5 h against 4 L of buffer B and then was loaded onto a Sephadex G-200 column (1.5 x 30 cm) that was previously equilibrated with buffer B. The enzyme was eluted with 120 mL linear gradient of 0 to 1 N NaCl in buffer B and one major peak was observed. Solid ammonium sulphate was added to the “peaked pooled fractions” to form 0 to 35%, 35 to 70% and 70 to 90% saturation fractions respectively. Each fraction was dialyzed separately against buffer B with two changes for 24 h and measured for NAD-IDH activity. The 35 to 70% saturation fraction was found to have a high enzyme activity and was layered onto a DEAE-Sephacel (0.7 x 20 cm) which was previously equilibrated with buffer B at a flow rate of 15 $mL.h^{-1}$.

Bound enzyme was eluted with 60 mL linear gradient (0 to 1 N NaCl in buffer B). Fractions (0.5 mL) containing NAD-IDH activity were pooled, dialyzed as before and applied onto a Sephacryl S-100 column (0.5 x 30 cm) equilibrated with buffer B at a flow rate of 15 $mL.h^{-1}$ and the enzyme was eluted with 100 mL linear gradient (0 to 1 N NaCl in the same buffer) and 1 mL fractions were collected. The pooled peak-activity fractions were dialyzed as before and then concentrated by ultrafiltration and kept at 4°C for immediate use or stored at -20°C.

Enzyme assay and protein determination

The NAD-IDH activity was determined in a 1 mL reaction containing buffer B, 0.5 mM $MnCl_2$ (or 1.0 mM $MgSO_4$), 1.5 mM NAD, 4 mM DL isocitrate, 0.5 mM ADP and the appropriate amount of the enzyme. All the assays were performed at 37°C in a final volume of 2.5 mL. The reaction was started by the addition of the isocitrate and followed by the increase in A_{340}. One unit of activity was defined as the amount of enzyme that catalyzed the production of 1 umole of NADH per mL of reaction mixture per min under the standard conditions. Specific activity is defined as units per mg of protein. All assays were performed in triplicate. Protein was estimated by the method of Bradford (1976) with BSA as a standard.

Enzyme kinetics

A kinetic analysis was done on the purified enzyme following Sephacryl S-100 chromatography. Determination of K_m values for the enzyme was carried out in 0.1 mM tris-HCl buffer, pH 7.5, and 1 mM $MgSo_4$ at different concentrations.

Gel electrophoresis

Sodium dodecyl sulfate-polyacrylamide gel electrophoresis (SDS-

PAGE) was performed as described by Laemmli et al. (1970) as modified by Maizel (1970) using 12% polyacrylamide gel. Proteins were located in the gel by staining with 0.1% (w/v) Coomassie brilliant blue R-250 in 25% (v/v) ethanol and 10% (v/v) acetic acid. NAD-IDH activity was located by running a separate lane with pooled active fractions from Sephacryl S-100 which was cut out from the gel before staining. The lane is cut horizontally into 0.25 mm pieces and submerged in buffer B and assayed for activity as in methods.

Estimation of native molecular mass

The molecular mass of NAD-IDH was estimated by SDS-PAGE. Protein markers of known sizes: ferritin from equine spleen (364kD), catalase from *Aspergillus niger* (240 kD), myosin from rabbit muscles (205 kD), B-galactosidase from *Escherichia coli* (116 kD), bovine serum albumin (67 kD), fumarase from porcine heart (48 kD), ovalbumin (45 kD) and cytochrome C (12.5 kD) were used as standards.

RESULTS

Purification

The purification of the enzyme is shown in Table 1. The NAD^+-dependent IDH was purified to near homogeneity (about 1216-fold) with specific activity of 2250 units.mg^{-1} and a recovery of 7.5%. DEAE-Sepharose, Sephadex G-200 and ammonium sulphate fractionation did remove most of the contaminating proteins (Table 1). The shape of the peak of Sephacryl S-100 suggested heterogeneity of the enzyme, or that the enzyme consists of several units (Figure 1). The active fractions of the column preserved in -20°, so that little loss of enzyme activity occurred.

Optimum pH

The pH optimum of NAD-IDH was 7.5, but with the addition of ADP, the pH optimum shifted to the alkaline side and becomes 8.2.

Optimum temperature

The optimum temperature was at 37°C, but dropped quickly and disappeared completely at 50°C.

Enzyme stability

The enzyme in its purified form was stable up to 30 min at room temperature and for 12 h at 4°C. The addition of 20% glycerol to the enzyme stabilized the enzyme substantially (up to 21 h at 4°C), and up to three weeks at -20°C, but any higher concentration will interfere with the chromatography steps. BSA (up to 10%) did not stabilize or activate the enzyme, and shows no effect at all.

Divalent metals effects

The enzyme showed activity in the absence of any divalent metal ions, but Mn^{+2} was a better activator than Mg^{+2} at lower concentrations (0.5 mM), but it would inhibit the enzyme at higher concentrations (2 mM). Mg^{+2} did not inhibit the enzyme over a wide range of concentrations, so it was preferably used instead of Mn^{+2}. Cobalt would activat the enzyme slightly but other divalent ions would have inhibitory or no effect on it (Table 2).

Effects of substrates

ADP enhanced the activity of the enzyme by 60 to 80%, while AMP had no effect at all, but it inhibited some activity if mixed with ADP. GMP, GDP and GTP have no effect on the activity of NAD-IDH. A number of substrates and some intermediates of the TCA cycle (such as glutamate, fumarate, pyruvate, succinate and citrate) showed no stimulation effect on the enzyme. EGTA and EDTA addition inhibited the enzyme by about 20%. For this reason, 1 mM Mg was used in all experiments with 0.5 mM ADP.

Estimation of molecular mass

The pooled active fractions from 35 to 70% desalted ammonium sulphate fraction, DEAE-Sephacel and Sephacryl S-100 were electrophoresed on SDS-PAGE at pH 7.5. Several bands were extending from top to bottom. Four bands were appeared in Sephacryl S-100 lanes (lanes 3, 4, Figure 2) which had strong NAD-IDH activities. These activities were identified by running a separate lane with pooled active fractions from Sephacryl S-100 which was cut out from the gel before staining. The lane is cut horizontally into 0.25 mm pieces and submerged in 0.1 M tris-HCl buffer, pH 7.5 and assayed for activity as in methods. By comparing the positions of the four bands with standards used as described in methods, NAD-IDH from Sephacryl S-100 was clearly a tetramer with subunits of 80,000 and the native molecular mass is about 320,000.

Inhibition by ATP and NADH

ATP and NADH inhibited the enzyme competitively according to Lineweaver-Burk plot (1934). The value of Ki was measured to be 1.8 and 0.6 mM for ATP and NADH respectively under standard conditions (Figures 3 and 4).

Table 1. Purification of NAD^+-IDH from human kidney.

Purification step	Volume (mL)	Total activity (units)	Total protein (mg)	Specific activity ($unit.mg^{-1}$)	Purification (-fold)	Yield (%)
Mitochondrial preparation	20	120	65.0	1.85	1	100
DEAE-Sepharose	30	96	5.2	18.5	10	80.0
Sephadex G-200	45	65	0.8	81.2	44	54.1
35 to 70% $(NH_4)_2SO_4$ fraction	10	43	0.1	430	232	35.8
DEAE-Sephacel	25	15	0.01	1500	811	12.5
Sephacryl S-100	10	9	0.004	2250	1216	7.5

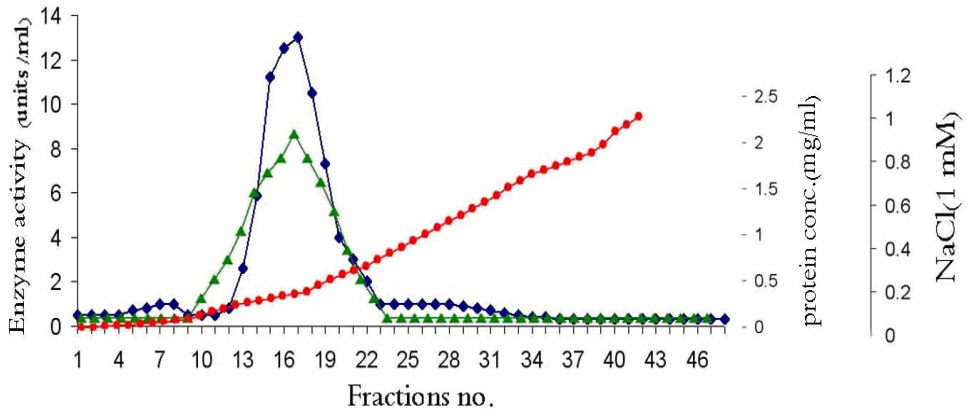

Figure 1. Elution profile of NAD-IDH activity from Sephacryl S-100 column (●) with its protein profile (▲) and the linear gradient of sodium chloride (0-1mM) (■).

Table 2. Effect of divalent metal ions on NAD^+-IDH activity from the pooled fractions from Sephacryl S-100.

Ion (mM)	Effect (100%)
Control	100
Manganese (0.5)	140
Manganese (1.0)	320
Manganese (1.5)	110
Manganese (2.0)	70
Magnesium (0.5)	120
Magnesium (1.0)	250
Magnesium (1.5)	180
Magnesium (2.0)	130
Cobalt (0.5)	130
Cobalt (1.0)	170
Cobalt (1.5)	130
Cobalt (2.0)	110
Copper (0.5)	60
Copper (1.0)	50
Calcium (0.5)	100
Calcium (1.0)	100
Zinc (0.5)	40
Zinc(1.0)	17

Effect of ADP on NAD-IDH

It seemed possible that a homotropic cooperative effect of isocitrate in either the absence or presence of ADP might occur if concentrations of NAD-IDH were limiting. A hill plot was plotted with different amounts of isocitrate and fixed amounts of NAD-IDH. Straight parallel lines with slopes approaching a value of less than 1 were obtained with or without ADP. All the values of the slopes were less than 1 indicated that a cooperative effect of isocitrate had not been caused by changes of NAD-IDH concentration (Monod et al., 1963; Jacob et al., 2005). A lineweaver-burk plot was plotted either with different amounts of isocitrate and a fixed amount of NAD-IDH (Figure 5), or different concentrations of NAD-IDH and fixed concentration of isocitrate (Figure 6) in the absence (top) or presence (bottom) of ADP. The plots gave patterns of intersecting straight lines, indicated no deviation from Michaelis-type kinetics under these conditions for either isocitrate or NAD-IDH with the kidney enzyme. In the absence of ADP, the increased concentrations of NAD-IDH decreased the Km of isocitrate while the increased levels of isocitrate lowered the Km of NAD-IDH.

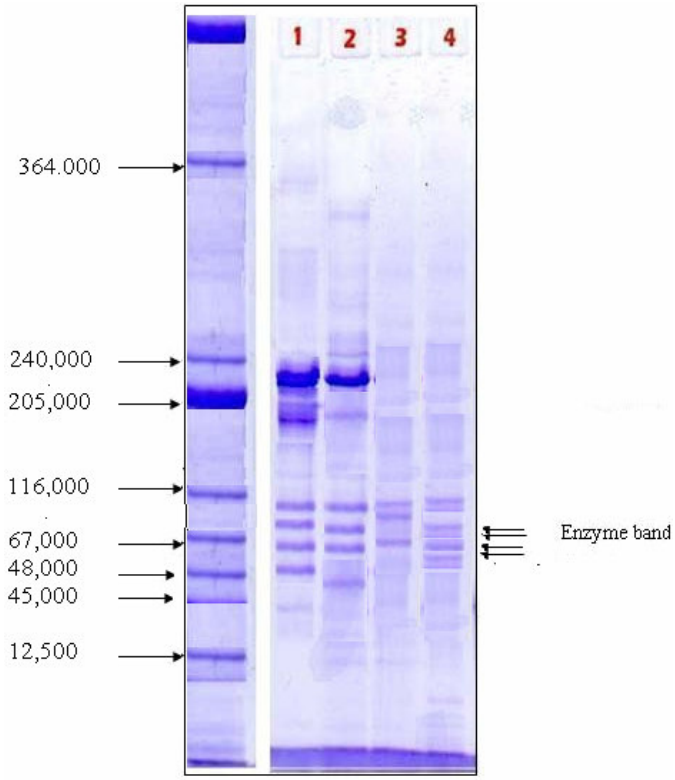

Figure 2. SDS-polyacrylamide gel with four lanes; lane 1, A 35 to 70% desalted ammonium sulphate fraction, lanes 2, the pooled peaked fractions from DEAE-Sephacel column, lanes 3, 4, the pooled peaked fractions from Sephacryl S-100. The arrows indicate the bands that show NAD-IDH activity.

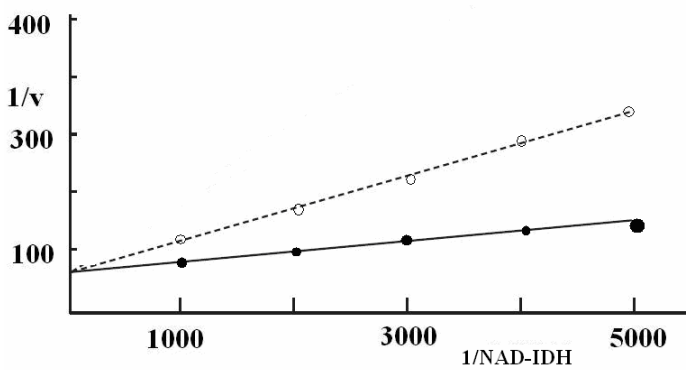

Figure 3. The effect on NAD-IDH in the presence (○) or absence (●) of ATP. The incubation mixture is as described under methods. NAD concentrations are varied while ATP concentration is fixed.

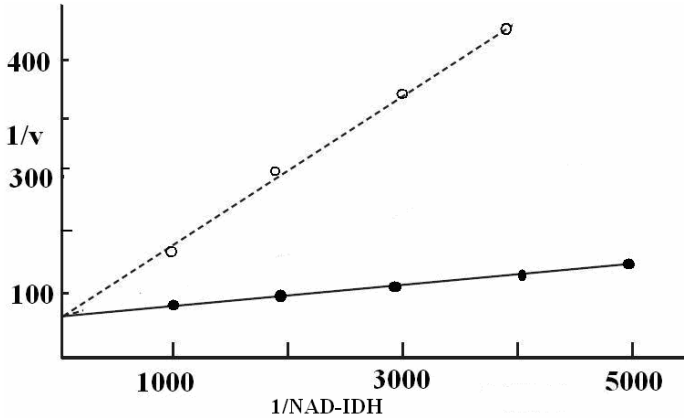

Figure 4. The effect on NAD-DH in the presence (○) or absence (●) of NADH. The incubation mixture is as described under methods. NAD concentrations are varied while NADH concentration is fixed.

The values of Km of either isocitrate or NAD-IDH were lowered further in the presence of ADP. The values of limiting Michaelis constants of isocitrate and NAD-IDH were calculated by the graphic method of Dalziel (1957) for two-substrates system where $Ø_1$, $Ø_2$, and $Ø_3$, are substituted by $Ø_{NAD\text{-}IDH}$, $Ø_{IC}$ and $Ø_{NAD.IC}$ (IC represents isocitrate):

$$e/V_0 = Ø_0 + Ø_1/[S_1] + Ø_2/[S_2] + Ø_3/[S_1][S_2]$$
$$e/V_0 = Ø_0 + Ø_{NAD\text{-}IDH}/[S_1] + Ø_{IC}/[S_2] + Ø_{NAD.IC}/[S_1][S_2]$$

A secondary plot was made of the intercepts at the ordinate (Figure 7, top) and the slopes (Figure 7, bottom) of the primary plots (Figures 5 and 6) against the reciprocals of the concentrations of isocitrate (or NAD-IDH). The value, furthermore, of the constants $Ø_0$, $Ø_{IC}$, $Ø_{NAD\text{-}IDH}$ were affected very little by the presence of ADP, even when ADP caused a marked decrease in the values of the complex constant $Ø_{NAD.IC}$ (Figure 7, bottom). Therefore, the values of V_{max}, K_{IC} and $K_{NAD\text{-}IDH}$ had been calculated and the maximal velocities K_{IC} and $K_{NAD\text{-}IDH}$ were essentially unaffected by ADP (K_{IC} = 0.32 mM and 0.26 nM, $K_{NAD\text{-}IDH}$ = 0.06 mM in the absence and presence of ADP respectively). However, the values of the ratios of the constants $Ø_{NAD.IC}/ Ø_{IC}$ and $Ø_{NAD.IC}/ Ø_{NAD\text{-}IDH}$ were 4 to 7 folds larger in the absence of ADP.

DISCUSSION

NAD-IDH had been purified from the mitochondria of human kidney 1216-fold with a total recovery of 7.5%. The combination of the affinity chromatography with the anion-exchange matrix allowed obtaining a preparation of high purity, and most contaminated proteins were removed. The shape of the peak from Sephacryl S-100 suggested that the enzyme consisted of four subunits. This observation was confirmed by SDS-PAGE which show that only four bands of protein from Sephacryl S-100 column had strong NAD-IDH activities. The enzyme

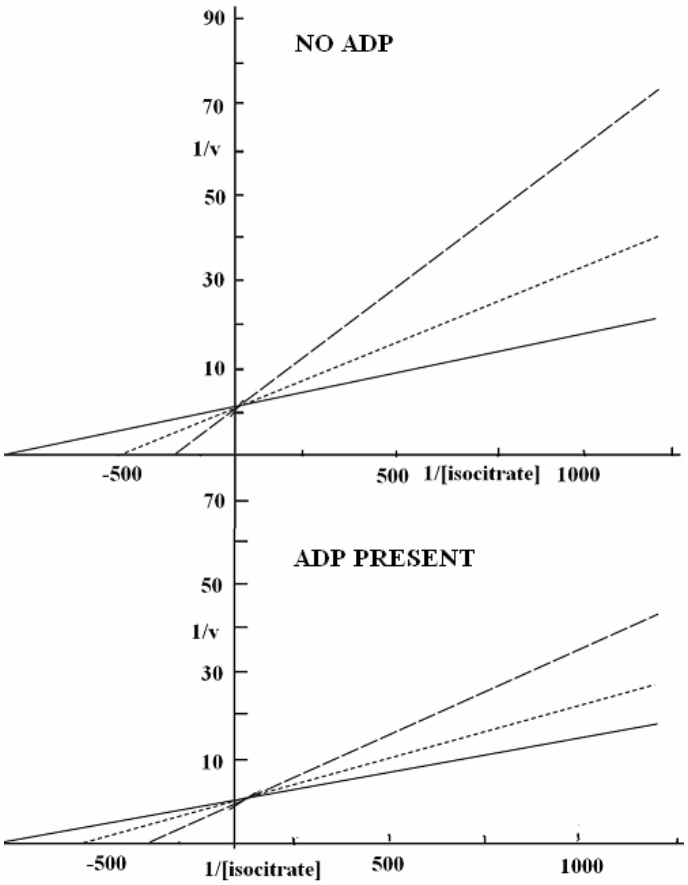

Figure 5. Primary plots of velocity which are using isocitrate concentrations at varying levels of NAD (0.5, 1.0 and 1.5 Mm) in the absence (top) and presence (Bottom) of ADP. The reactions mixture is described under methods.

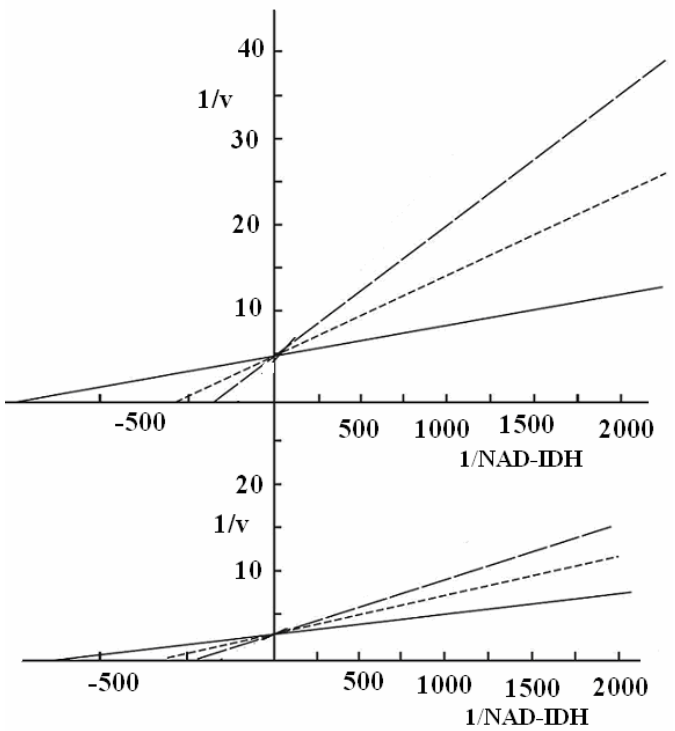

Figure 6. Primary plots of velocity which are using NAD concentrations at varying levels of isocitrate (0.5, 1.0 and 1.5 Mm) in the absence (top) and presence (bottom) of ADP. The reactions mixture is described under methods.

seemed to be a tetramer with four subunits of about 80,000 kD and a native molecular mass of about 320,000. These results agreed to some extents with results obtained from previous NAD-IDHs purifications such as Ehrlich et al. (1981), Shorrosh and Dixon (1992), Alvarez-Villafane et al. (1996), Cornu et al. (1996), Bzymek and Colman (2007) and Dangee et al. (2008).

AMP could not activate NAD-IDH enzyme, even when some researchers claimed the opposite (Hathaway and Atkinson, 1963; Plaut and Aogaichi, 1968). The author believed that such activation was of doubtful physiological significance since the concentration required differed by several orders of magnitude from that present in tissues. The response of NAD-IDH in human kidney to varying concentrations of isocitrate and NAD-IDH corresponded essentially to the kinetics of two substrate reactions observed with a number of other pyridine nucleotide dehydrogenases. ADP did not modify the limiting Michaelis constants of NAD-IDH and isocitrate, but had a marked effect on the slopes of the lines of Lineweaver Burk plots (Figures 5 and 6) and the secondary plots derived there from (Figure 7). Thus ADP lowered and decreased the ratios of the complex constants $Ø_{NAD\cdot IC}/ Ø_{IC}$ and $Ø_{NAD\cdot IC}/ Ø_{NAD\text{-}IDH}$ and the symmetry of the effect of ADP on values of $Ø_{NAD\cdot IC}$ (Figure 6) seemed to imply that the nucleoside diphosphate did not preferentially modify one of the interacting sites for substrate and coenzyme over the other.

The significance of the complex constants represented by the ratios $Ø_{NAD\cdot IC}/ Ø_{IC}$ and $Ø_{NAD\cdot IC}/ Ø_{NAD\text{-}IDH}$ were somewhat difficult to evaluate. Hartong et al. (2008) had shown that a number of pyridine nucleotides linked dehydrogenasess followed an ordered sequential reaction pathway in which the addition of coenzyme to the enzyme preceded interaction with substrate (Lee, 2002). The lack of reversibility of the NAD-IDH reaction precluded a definitive kinetic analysis the intersection points of the primary plots were calculated (Figures 4 and 5) according to the method of Frieden (2007). The values were quite comparable to those calculated from those of the rations of the ØΦ constants (Abiko et al., 2005). Inhibition of NAD-IDH by NADH competitively was consistent with an ordered sequential mechanism of addition of NAD-IDH followed by oxidizing substrate in

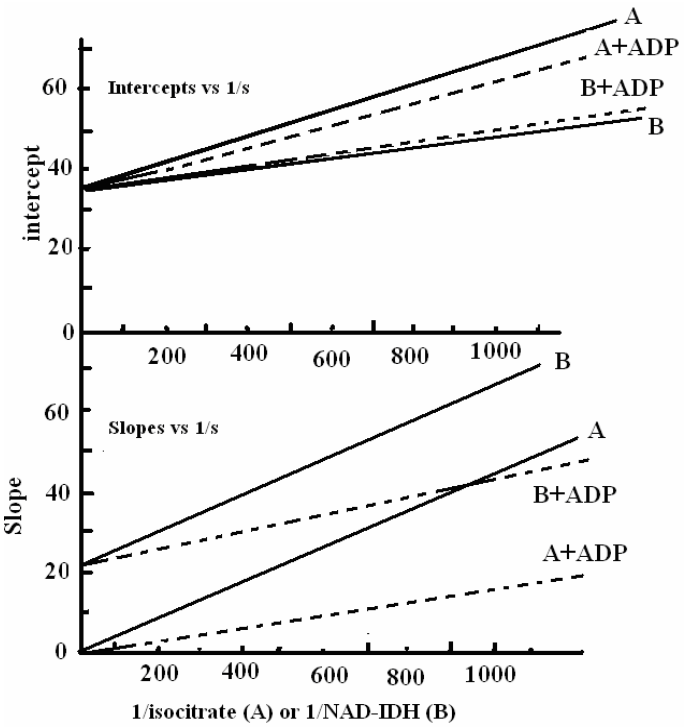

Figure 7. Secondary plots of intercepts (top) and slopes (bottom) of values with respect to the reciprocal of NAD or isocitrate concentration.

which NADH is the last product detached from the enzyme. The oxidizing and reducing forms of the pyridine nucleotide competed, presumably, for the same site on the enzyme and on this case a similar effect of ADP on the dissociation constants of NAD-IDH and NADH may be expected (Bzymek and Colman, 2007; Dangee et al., 2008). Other possibility was that the interaction of the enzyme with NADH may cause the protein to assume a conformation in which a catalytic site was no longer affected by ADP while such interaction still occurs in the enzyme-NAD complex (Lancien et al., 1999). In terms of physiological role of the human kidney, it was significant that isocitrate influenced the value of km of NAD-IDH at limiting substrate and coenzyme concentrations and vice versa. In addition, ADP lowered both constants (Weiss et al., 2000).

The activity of NAD-IDH was influenced by a number of factors such as interacting substrates such as isocitrate and NADH, and the divalent activators (Mn^{+2} or Mg^{+2}). ADP influenced the enzyme also, while ATP and NADH inhibited it competitively. The intermediates of TCA had no effect which suggests that lack of reversibility of the reaction may be due partly to poor binding of TCA intermediates to the enzyme in addition to the product inhibition by ATP (or NADH). Future studies are aiming to the cloning of the gene and required to understand the regulatory mechanism of NAD-IDH.

ACKNOWLEDGMENTS

The author is grateful for the valuable assistance of Dr. Hasan A. Abder-Rahman, PhD, JMC from Forensic Medicine and Pathology Department, Faculty of Medicine, University of Jordan, Amman, Jordan. My gratitude to professor Musa H. Abu Zarga, Department of Chemistry, Faculty of Science, The University of Jordan for his valuable advices. I am debited to Professor Julia Bejar Alvarado, Department of Cellular Biology, Genetics and Physiology, University of Malaga and Professor Manchikatla Venkat Rajam, Department of Genetics, University of New Delhi India for their valuable suggestions and criticism in kinetics studies. My deep gratitude is to the staff in laboratory 1, College of Pharmacy, Al-Zaytoonah University for their cooperation and help.

REFERENCES

Abiko T, Obara M, Ushioda A, Hayakawa T, Hodges M, Yamaya T (2005). Localization of NAD-Isocitrate Dehydrogenase and Glutamate Dehydrogenase in Rice Roots: Candidates for Providing Carbon Skeletons to NADH-Glutamate Synthase. Plant Cell Physiol., 46(10): 1724-1734.

Alvarez-Villafañe E, Soler J, del Valle P, Busto F, de Arriaga D (1996). Two NAD^+-isocitrate dehydrogenase forms in *Phycomyces blakesleeanus*: induction in response to acetate growth and characterization, kinetics, and regulation of both enzyme forms. Biochemistry, 35: 4741-4752.

Bradford MM (1976). A rapid and sensitive method for the quantization of microgram quantities of protein utilizing the principle of protein-dye binding. Anal. Biochem., 72: 248-254.

Bzymek KP, Colman RF (2007). Role of α-Asp181, β-Asp192 and γ-Asp190 in the Distinctive Subunits of Human NAD-Specific Isocitrate Dehydrogenase. Biochemistry, 46: 5391-5397.

Chen RD, Gadal P (1990). Structure, function and regulation of NAD and NADP dependent isocitrate dehydrogenases in higher plants and in other organisms. Plant Physiol. Biochem., 28: 411-427.

Chen R, Jeong SS (2000). Functional prediction, identification of protein orthologs and paralogs. Protein Sci., 9: 2344-2353.

Cornu S, Pireaux JC, Gerard J, Dizengremel P (1996). NAD(P) dependent isocitrate dehydrogenases in mitochondria purified from Picea abies seedlings. Physiol. Plant., 96: 312-318.

Dalziel K (1957). Initial steady state velocities in the evaluation of enzyme-coenzyme substrate reaction mechanism. Acta Chem. Scand., 11(1): 706-723.

Dange M, Hartong DT, McGee TL, Berson EL, Dryja TP, Colman RF (2008). Mutations of the beta-subunit of human NAD-specific isocitrate dehydrogenase in patients with Retinitis pigmentosa. FASEB J., 22: 1032.1

Ehrlich RS, Hayman S, Ramachandran N, Colman RF (1981). Re-evaluation of molecular weight of pig heart NAD-specific isocitrate dehydrogenase. J. Biol. Chem., 256: 10560-10564.

Frezza C, Cipolat S, Scorrano L (2007). Organelle isolation: functional mitochondria from mouse liver, muscle and cultured fibroblasts. Nat. Prot., 2: 287-295

Frieden C (2007). Protein aggregation processes: In search of the mechanism. Protein Sci., 16: 2334-2344.

Gregg C, Kyryakov P, Titorenko VI (2009). Purification of Mitochondria

from Yeast Cells. http//www.jove.com/index/details.stp?id=1417. JOVE: J. visual. Exp., p. 30.

Hartong DT, Dange M, McGee TL, Berson EL, Thaddeus P Dryja, Colman RF (2008). Insights from retinitis pigmentosa into the roles of isocitrate dehydrogenases in the Krebs cycle. Nat. Genet., 40: 1230-1234.

Hathaway JA, Atkinson DE (1963). The effect of adenylic acid on yeast nicotinamide adenine dinucleotide isocitrate dehydrogenase, a possible metabolic control mechanism. J. Biol. Chem., 238: 2875-2881.

Jacob F, Perrin D, Sánchez C, Monod J, Edelstein S (2005). The operon: a group of genes with expression coordinated by an operator. C.R. Acad. Sci. Paris, 250(1960): 1727-1729". Comp. Rendus Biol., 328(6): 514-520.

Karlstrom M, Stokke R, Steen IH, Birkeland NK, Ladenstein R (2005). Isocitrate dehydrogenase from the hyperthermophile Aeropyrum pernix: X-ray structure analysis of a ternary enzyme-substrate complex and thermal stability. J. Mol. Biol., 345: 559-577.

Kurnick NB, Mirsky AE (1950). Methyl green pyronin II. Stoichiometry of reaction with nucleic acids. J. Cell Biol., 33(3): 265-270.

Laemmli UK (1970). Cleavage of structural proteins during the assembly of the head of bacteriophage T4. Nature, 227: 680-685

Lancien M, Ferrario-Méry S, Roux Y, Bismuth E, Masclaux C, Hirel B, Gadal P, Hodges M (1999). Simultaneous Expression of NAD-Dependent Isocitrate Dehydrogenase and Other Krebs Cycle Genes after Nitrate Resupply to Short-Term Nitrogen-Starved Tobacco. Plant Physiol., 120: 717-726.

Lee P, Colman RF (2002). Implication by site-directed mutagenesis of Arg314 and Tyr316 in the coenzyme site of pig mitochondrial NADP-dependent isocitrate dehydrogenase. Arch. Biochem. Biophys., 401(1): 81-90.

Lineweaver H, Burk D (1934). The determination of the enzyme dissociation constants. J. Am. Chem. Soc., 56: 658-666.

Maizel JV (1971). Polyacrylamide gel electrophoresis of viral protein. In: Maramorosch K, Koprowshi H (Eds.). Methods in Virology 5, Academic Press, New York, pp. 179-246.

Monod J, Changeux J (1963). Allosteric proteins and cellular control systems. J. Mole. Boil., 6: 306-329.

Oliver DJ, McIntosh CA (1995). The biochemistry of the mitochondrial Matrex. In CS Levings III, IK Vasil, eds, The Molecular Biology of Plant Mitochondria: Advances in Cellular and Molecular Biology of Plants. Kluwer Academic Publishers, Dordrecht, Netherlands, 3: 237-280.

Plaut GWE, Gabriel JL (1983). Role of isocitrate dehydrogenase in animal tissue metabolism. In: Lennon DLF, Stratman FW, Zahlten RN eds. Biochemistry of metabolic processes. Amsterdam Elsevier Sci., pp. 129-142.

Shorrosh BS, Dixon RA (1992). Molecular characterization and expression of an isocitrate dehydrogenase from alfalfa (*Medicago sativa* L.). Plant Mol. Biol., 20: 801-807.

Tezuka T, Laties GG (1983). Isolation and characterization of inner-membrane associated and matrix NAD-specific isocitrate dehydrogenase in potato mitochondria. Plant Physiol., 72: 959-963.

Wadano A, Miura K, Ihara H, Kondo N, Taniguchi M (1989). Purification and some properties of Isocitrate dehydrogenase of a blowfly *Aldrichina graham*. Comp. Biochem. Physiol., 94B: 189-194.

Weiss C, Zeng Y, Huang J, Sobocka MB, Rushbrook JI (2000). Bovine NAD+-dependent isocitrate dehydrogenase: alternative splicing and tissue-dependent expression of subunit 1. Biochemistry, 39(7): 1807-1816.